SPE 74367

CO_2 Injection for Enhanced Gas Production and Carbon Sequestration

Curtis M. Oldenburg and Sally M. Benson SPE, Lawrence Berkeley National Laboratory

Abstract

Analyses suggest that carbon dioxide (CO_2) can be injected into depleted gas reservoirs to enhance methane (CH_4) recovery for periods on the order of 10 years, while simultaneously sequestering large amounts of CO_2. Simulations applicable to the Rio Vista Gas Field in California show that mixing between CO_2 and CH_4 is slow relative to repressurization, and that vertical density stratification favors enhanced gas recovery.

Introduction

Although the idea of injecting carbon dioxide (CO_2) into depleted natural gas reservoirs for carbon sequestration with enhanced gas recovery (CSEGR) has been around for more than ten years[1,2], and independent analyses have been carried out that suggest the feasibility of the process[3,4], CSEGR has yet to be implemented commercially or even tested in the field. Among the reasons for this is concern about mixing of CO_2 with native methane (CH_4) gas and the corresponding degradation of value of the remaining natural gas. Our previous analysis of the physical processes involved in CSEGR suggested that mixing would be limited because of the high density and viscosity of CO_2 relative to CH_4.[4] Furthermore, our simulations suggested that CSEGR could enhance gas production by a factor of five over 20 years relative to continued primary recovery over the same period for the large Rio Vista Gas Field in California. These prior simulations were done in idealized reservoirs using simple relations for gas mixture properties.

The purpose of this paper is to show additional and more detailed analyses that extend and amplify our prior findings to provide a broader scientific foundation for pilot testing and ultimate large scale deployment of CSEGR. These analyses include a discussion of physical properties of gas mixtures in the system CO_2-CH_4, and simulations of the effects of permeability heterogeneity and vertical stratification in a three-dimensional five-spot CSEGR scenario.

Background and Prior Work

As shown schematically in Figure 1 for a single power plant and gas reservoir, CSEGR is the injection of CO_2 into depleted natural gas reservoirs for carbon sequestration with enhanced gas recovery. Because they have held large quantities of natural gas over geologic time scales, depleted gas reservoirs offer a proven integrity against gas escape and large available capacity for carbon sequestration, estimated at 140 GtC (Gigatonnes Carbon) worldwide[5], and 10-25 GtC in the United States[6]. There do not seem to be any technical barriers to CO_2 injection, although there are certainly costs associated with the injection of a highly corrosive gas such as CO_2[7].

Despite the vast potential for carbon sequestration in depleted gas reservoirs, CSEGR has not been tested in the field due apparently to the high present cost of CO_2 and infrastructure, concerns about excessive mixing, and the high primary recovery rates of many gas reservoirs[8]. These arguments notwithstanding, CSEGR may offer other benefits including pressure support in the reservoir to prevent subsidence and water intrusion. Furthermore, in the future companies may be paid to dispose of CO_2 as a greenhouse gas as opposed to buying it as a commodity, thus reversing the economic barrier.

As for mixing, the injection of CO_2 enhances gas recovery through both displacement, analogous to a water flood in oil recovery, and by repressurization of the remaining CH_4. Repressurization of gas effectively concentrates the CH_4 mass at distances far removed from the injection location without contamination by the injected gas. Furthermore, as discussed in our prior publication[4] and below, the high density and viscosity of CO_2 relative to CH_4 can be exploited to avoid excessive mixing in the reservoir. In addition, the schematic of CSEGR for a coupled gas-fired power plant and gas reservoir shown in Figure 1 emphasizes that comanagement between the producing reservoir and the power plant may allow for greater acceptance of mixed CO_2-CH_4 gases as powerplant feedstock, in addition to allowing flexibility in gas production in response to fluctuating power demands.

Finally, while high primary recovery of natural gas would seem to trivialize the EGR component of CSEGR, the fact is that large amounts of gas remain in large depleted gas reservoirs. If the choice is between idling wells and abandoning the field versus further productive use of the reservoir in terms of energy production and carbon sequestration, it would appear that CSEGR should be given a fair evaluation.

The first published simulation results of CO_2 injection into natural gas reservoirs for CSEGR considered injection into a two-dimensional five-layer dipping reservoir typcial of Dutch gas reservoirs[1]. They found limited EGR due to early breakthrough of CO_2 to production wells. Simulation results from the same study were used for analyzing the feasibility of hydrogen production, a process in which limited CO_2 mixing with the natural gas is acceptable[3]. While CH_4-CH_4 mixing has been documented in gas reservoirs in Yugoslavia by carbon isotopic analyses[9], inert gas cushions appear not to mix excessively in natural gas storage projects in France[10,11,12]. Thus the question is open as to whether or not excessive gas mixing will occur in gas reservoirs in general, and whether operational methods can be employed to control gas mixing.

Recent simulation results of CSEGR were presented that focused on the large Rio Vista Gas Field in California[4]. Results from this study showed that CSEGR could produce approximately five times as much gas over the next 20 years as compared to a projection based on existing primary production. In addition, we estimated that the Rio Vista Gas Field could store for the next 80 years all of the CO_2 produced by the 680 MW Antioch gas fired power plant located 20 km to the southwest. These simulations assumed a two-dimensional reservoir, with homogeneous anisotropic permeability, and simple mixing relations for physical properties in the mixed gas system. In the current study, real gas mixture properties in the system CH_4-CO_2-H_2O are used with more realistic reservoir conditions, including a three-dimensional five-spot domain, to corroborate and further demonstrate the physical processes that make CSEGR favorable.

Physical Properties

The physical properties of CO_2 and CH_4 at reservoir conditions strongly favor CSEGR. Shown in Figure 2 is the phase diagram for CO_2 indicating that supercritical conditions will prevail in typical gas reservoirs. As can be seen in Figures 3 and 4 by comparing end-member properties along either vertical axis, pure CO_2 is much denser and more viscous than pure CH_4 in gas reservoirs. CO_2 injectivity will be high due to its low absolute viscosity relative to water, for example, while having large density that will tend to underride existing gas. Furthermore, the relatively larger viscosity of CO_2 will make for a favorable mobility ratio displacement of CH_4 with diminished tendency to interfinger and mix with the displaced CH_4. Thus the density and viscosity differences between pure CO_2 and CH_4 favor CSEGR by decreasing mixing. Also shown in Figures 3 and 4 are the density and viscosity of CO_2-CH_4 mixtures as calculated in our own simulator (TOUGH2/EOS7C) and NIST14[13,14] for verification. Where discrepancies were seen for the viscosity of pure CO_2, we have also plotted data[15] that show both models to be good approximations.

In the gas reservoir simulations presented below, gas property calculations include the effects of water vapor as it partitions into the gas phase from connate water forming the gas mixture system CH_4-CO_2-H_2O. Verification of physical property calculations in the system CH_4-CO_2-H_2O was done by comparing results against published data[16,17] and models[18,14]. Agreement is good between our mixing models and other published work for density, viscosity, and enthalpy departures in the real gas mixtures at all relevant pressures and temperatures.

Simulation Methods

We use TOUGH2/EOS7C for simulating nonisothermal multiphase and multicomponent flow and transport in gas reservoirs. As an extension of the intergral finite difference code TOUGH2[19], EOS7C considers five mass components (water, brine, CO_2, gas tracer, CH_4) and heat. EOS7C incorporates a Peng-Robinson equation of state for calculating real gas mixture properties (density and enthalpy departures) across the entire range of relevant pressures and temperatures. Accurate gas mixture viscosities are calculated[20,21], as are the solubilities of gaseous components[22] to include effects of solubility trapping by connate water. Because it is a module of TOUGH2, full multiphase capabilities are simulated in EOS7C that can be used to model water table displacements and water drive.

Rio Vista Revisited

The Rio Vista Gas Field, located 75 km NE of San Francisco, CA, is the largest onshore gas field in California[23,24]. The alternating layers of sands and shales deposited in deltaic and marine environments form a faulted dome-shaped structure extending over an area 12 km by 15 km. The Domengine formation is the most productive reservoir in the Rio Vista Gas Field and occurs at an average depth of 1150 m to 1310 m with an average net thickness of 15 m to 100 m. Under production for many decades, pressures have declined from initial values near 125 bars and the current $\sim 10^7$ Mcf yr^{-1} ($\sim 1.9 \times 10^8$ kg yr^{-1}) gas production rate is a small fraction of the peak rate of $\sim 1.6 \times 10^8$ Mcf yr^{-1} ($\sim 3.1 \times 10^9$ kg yr^{-1}). High water cuts or low production have led to idling of many wells or producing them at very low rates. The Rio Vista Gas Field is approximately 20 km from a 680 MW gas-fired power plant that produces 2.2×10^9 m^3 (4.15×10^9 kg) of CO_2 per year. As concluded in the earlier study[4], the Rio Vista Gas Field appears to be a good candidate for CSEGR.

Building on our prior Rio Vista simulations[4], we have extended the work to include CO_2 injection into a heterogeneous two-dimensional reservoir (1/16 of the Rio Vista system) while monitoring the pressure and breakthrough curves at four locations updip from the injection point (Figure 5). We discretized the domain into 660 (33 x 20) gridblocks 200 m x 5 m in the Y- and Z-directions, respectively. The reservoir properties and conditions are given in Table 1. We present results for one realization of a statistically generated permeability field produced by a simulated annealing algorithm that resulted in subhorizontal bodies with two orders of magnitude variation in permeability (Figure 6a). The mass fraction of CO_2 in the gas and gas density are shown along with gas velocity vectors in Figures 6b and 6c after 10 years of CO_2 injection. The effects of variable permeability can clearly be seen in Figure 6 as gas moves faster through the higher permeability bodies. In general, we observed in simulations of numerous realizations (not presented here) that the effect of permeability heterogeneity is to accelerate CO_2 breakthrough, with faster breakthrough for larger permeability variations. The reason for this is that the injected CO_2 finds fast flow paths. Nevertheless, breakthrough is much slower than repressurization as discussed below.

We show in Figure 7 the pressure and breakthrough curves at various locations across the field as a function of time. As shown in Figure 7, pressure rises within the first year (1999) at all four monitoring locations well before any CO_2 mass is transported these distances. In essence, CO_2 injection causes repressurization of the whole reservoir with contamination by CO_2 restricted to about one half of the domain after five years. As shown in Figure 7, breakthrough occurs at Y = 3100 m after about one year of injection; after five years, a well at this location would produce nearly pure CO_2. The breakthrough at Y = 6500 m occurs after approximately 12 years of injection, but CO_2 does not comprise more than 50% of the produced gas even after 21 years. Subsequent to the first year repressurization, pressures at each monitoring well remain approximately constant until a significant fraction of CO_2 reaches each well whereupon pressure begins to increase.

During this 21-year period, gas recovery is significantly enhanced relative to a non-injection projection as shown in Figure 8. In this simulation, six times more gas is produced over 21 years (5.7×10^7 Mcf, 1.1×10^9 kg) relative to a projection that involves continuing primary production with no CO_2 injection (9.4×10^6 Mcf, 1.8×10^8 kg) from this 1/16 model reservoir. This simulation is for a single realization of permeability heterogeneity and is for a two-dimensional reservoir idealized in many ways. Nevertheless, the calculations suggest that CSEGR can potentially sequester all of the CO_2 produced by a large gas-fired power plant while improving production of high-quality natural gas for a period of at least 10 years.

Three-Dimensional Five Spot

A further extension of our simulation work was made to include three-dimensional effects that show that different injection and production elevation intervals can be exploited to minimize CO_2 production. We show in Figure 9 a schematic of a five spot geometry, where our simulation domain as outlined by the heavy lines is in one-quarter of the five spot pattern. The quarter five spot domain is 50 m thick by 200 m x 200 m, thus approximating a symmetry element from a 40-acre well pattern in which CO_2 is injected at the center well and CH_4 is produced from the surrounding four wells. We discretized the quarter five spot domain into 4410 gridblocks (10 in the vertical, 21 x 21 in the horizontal directions).

For this study, we specified the single-well CH_4 production by dividing the current Rio Vista CH_4 production by an assumed 320 wells (16 wells/mi^2 x 20 mi^2) and increasing this by 50% to account for EGR. We similarly divided the Antioch power plant CO_2 production rate by 320 assuming it would be injected equally in wells distributed across the field. We then specified gas production to occur from the top 10 m of the formation, while the CO_2 injection occurs over the bottom 10 m of the formation. The idea here is to exploit the large density difference between CO_2 and CH_4 to effectively fill the reservoir from the bottom up. Properties of the reservoir and injection rates are specified in Table 2. Although some of the properties were chosen based on Rio Vista, this is intended to be a generic quarter five spot simulation applicable to large gas fields in general.

The gas velocity and CO_2 mass fraction are shown in Figure 10 after eight years of injection when CO_2 breakthrough is just starting. As shown, the CO_2 is distributed throughout the bottom portion of the three-dimensional domain even though it was injected at the SW corner (X = Y = 0). Thus, the sweep of CO_2 is from the SW and below toward the northeast (X = Y = 200 m) and upward. This simulation shows the mixed zone after eight years is approximately 15 m thick, where mixing is due to molecular diffusion and numerical dispersion in this relatively coarsely gridded domain. Because the volumetric injection rate is larger than the specified constant production rate, the pressure in the reservoir steadily rises as CO_2 is injected from 50 bars initial pressure up to 67 bars after eight years. Actual EGR could be larger and associated CO_2 breakthrough faster if the production rate were larger. However, this simulation was carried out as CSEGR where a primary objective was the injection of large quantities of CO_2. Figure 11 shows the gas density to emphasize the strong density stratification present in the reservoir. This stratification helps delay CO_2 upconing into the production well.

As can be deduced from Figure 3, density stratification would be even larger for higher pressure reservoirs (e.g., P_0 = 101 bars), and larger mass injections of CO_2 could be accommodated in the reservoir by virtue of the three-fold increase in CO_2 density between 50 bars and 100 bars at 65 °C. Vertical mixing in such a system consisting of supercritical CO_2 at 300 kg m^{-3} and CH_4 at 50 kg m^{-3} would be limited by strong gravity effects.

Conclusions

We have extended our analysis of CSEGR through the use of accurate gas property models in simulations of CO_2 injections into heterogeneous and three-dimensional model depleted gas reservoirs. Our simulations show that significant amounts of CO_2 can be injected to produce significant quantities of additional natural gas. Furthermore, mixing in the gas reservoir is limited by the large density and viscosity of CO_2 relative to CH_4. These physical property differences become even larger at higher pressures, as CO_2 undergoes large changes in density and viscosity as pressures increase beyond the critical pressure of 73.8 bars. Permeability heterogeneity tends to accelerate breakthrough by the creation of fast flow paths. However, by injecting CO_2 at large distances from CH_4 production wells, one can take advantage of fast repressurization effects long before mass transfer allows CO_2 to contaminate produced gas even in a strongly heterogeneous system. Injecting CO_2 at relatively deeper levels in a reservoir while producing from higher levels will allow an operator to decrease CO_2 upconing and mixing. Mixing is inhibited by the strong density contrast that causes CO_2 to fill the reservoir from the bottom up, making an effective vertical and lateral sweep. We find that approximately eight years of EGR could be carried out in a 50 m thick reservoir in a field with 40-acre five spot patterns, while CO_2 injection could be carried out much longer as the reservoir is repressurized while shut in.

Acknowledgments

We thank George Moridis for development of the gas property module used in EOS7C. We also appreciate discussions with Karsten Pruess, Larry Myer, and Paul Witherspoon about gas reservoir processes, and review comments on the paper from Chris Doughty and Stefan Finsterle. This work was supported by the Assistant Secretary for Fossil Energy, Office of Coal and Power Systems through the National Energy Technology Laboratory, and by Lawrence Berkeley National Laboratory under Department of Energy Contract No. DE-AC03-76SF00098.

References

1. van der Burgt, M.J., J. Cantle, V.K. Boutkan, "Carbon dioxide disposal from coal-based IGCC's in depleted gas fields," Energy Convers. Mgmt., 33(5–8) (1992), 603.

2. Koide, H., Y. Tazaki, Y. Noguchi, M. Iijima, K. Ito, and Y. Shindo, "Underground storage of carbon dioxide in depleted natural gas reservoirs and in useless aquifers," Engineering Geology, 34 (1993) 175.

3. Blok, K., R.H. Williams, R.E. Katofsky, C.A. Hendricks, "Hydrogen production from natural gas, sequestration of recovered CO2 in depleted gas wells and enhanced gas recovery," Energy, 22 (2/3) (1997), 161.

4. Oldenburg, C.M., K. Pruess, and S.M. Benson, "Process modeling of CO2 injection into natural gas reservoirs for carbon sequestration and enhanced gas recovery," Energy and Fuels, 15 (2001) 293.

5. IEA (International Energy Agency), "Carbon Dioxide Utilization," IEA Greenhouse Gas R&D Programme, 1997; Table 6.

6. Reichle, D. et al., "Carbon sequestration research and development 2000," U.S. Department of Energy, DOE/SC/FE-1 (1999).

7. Bergman, P.D., E.M. Winter, and Z.-Y. Chen, "Disposal of power plant CO2 in depleted oil and gas reservoirs in Texas," Energy Conver. Mgmt, 38 Suppl. (1997) S211.

8. Stevens, S.H., V.A. Kuuskraa, J. Gale, and D. Beecy, "CO2 injection and sequestration in depleted oil and gas fields and deep coal seams: Worldwide potential and costs," Environmental Geosciences, 8(3) (2001) 200.

9. Buzek, F., "Carbon isotope study of gas migration in underground gas storage reservoirs," Czechoslavakia, Applied Geochemistry, 7 (1992) 471.

10. Carriére, J.F., G. Fasanino, and M.R. Tek, "Mixing in underground storage reservoirs," Soc. Petroleum Engineers SPE 14202 (1985).

11. Laille, J-P., J-E. Molinard, and A. Wents, "Inert gas injection as part of the cushion of the underground storage of Saint-Clair-Sur-Epte, France," Soc. Petrol. Engineers SPE 17740 (1988) 343.

12. De Moegen, H., and H. Giouse, "Long-term study of cushion gas replacement by inert gas," Soc. Petrol. Engineers SPE 19754 (1989) 487.

13. Magee, J.W., J.A. Howley, J.F. Ely, "A predictive model for the thermophysical properties of carbon dioxide rich mixtures," Research Report RR-136, Gas Processors Assoc., Tulsa OK (1994) 35 pp.

14. NIST (National Institute of Science and Technology), "NIST Database 14 Mixture Property Database, version 9.08," U.S. Department of Commerce (Oct. 1992).

15. Vargaftik, N.B., Y.K. Vinogradov, and V.S. Yargin, *Handbook of Physical Properties of Liquids and Gases, Third Edition*, Begell House, New York (1996) 1359 pp.

16. Joffrion, L.L. and P.T. Eubank, "Compressibility factors, densities, and residual thermodynamic properties for methane-water mixtures," J. Chem. Eng. Data, 34 (1989) 215.

17. Patel, M.R., and P.T. Eubank, "Experimental densities and derived thermodynamic properties for carbon dioxide-water mixtures," J. Chem. Eng. Data, 33 (1988) 185.

18. Duan, Z., N. Moller, and J. Weare. "An equation of state for CH4,CO2 and H2O II, Mixtures from 0 to 1000C and from 0 to 1000 bar." Geochim. Cosmochim. Acta, 56 (1992) 2619.

19. Pruess, K., C.M. Oldenburg, and G.J. Moridis, "TOUGH2 User's Guide Version 2.0," Lawrence Berkeley National Laboratory Report LBNL-43134 (November 1999), 197 pp.

20. Chung, T.-H., M. Ajlan, L.L. Lee, and K.E. Starling, "Generalized multiparameter correlation for nonpolar and polar fluid transport properties," Ind. Eng. Chem. Res. 27 (1988) 671.

21. Poling, B.E., J.M. Prausnitz, and J.P. O'Connell, *The properties of gases and liquids, fifth edition*, McGraw Hill, New York (2001).

22. Cramer, S.D., "The solubility of methane, carbon dioxide and oxygen in brines from 0 to 300 ˚C," U.S. Bureau of Mines: Report No. 8706 (1982) 16 pp..

23. Burroughs, E., Rio Vista Gas Field, "Summary of California oil fields, 53, No. 2-Part 2," State of California, Department of Conservation, Division of Oil and Gas (1967), 25.

24. Cummings, M. F., "Northern California oil and gas field production. Annual production and well data 1977-1998," State of California, Division of Oil, Gas and Geothermal Resources (1999).

25. van Genuchten, M.Th., "A closed form equation for predicting the hydraulic conductivity of unsaturated soils," Soil Sci. Soc. 44 (1980), 892.

Table 1. Relevant properties of Rio Vista model gas reservoir.

Property	Value	Units
Porosity	0.35	-
Mean *Y*-, *Z*-direction permeability	1.0 x 10^{-12}	m^2
Log permeability variance	0.33	-
Correlation length Y-direction	1000	m
Correlation length Z-direction	none	-
Capillary pressure m, S_{lr}, $1/\alpha$, P_{capmax}, S_{ls}	van Genuchten[25]; 0.2, 0.27, 8.4x10^{-4}, -10^5, 1.	 -, -, Pa^{-1}, Pa, -
Relative permeability liquid gas	 van Genuchten model Corey model (S_{gr} = 0.01)	 - -
Molecular diffusivity in gas, liquid	1.0 x 10^{-5}, 1.0 x 10^{-10}	$m^2\ s^{-1}$, $m^2\ s^{-1}$
Temperature	65	˚C
Initial pressure at water table	40	bars
CO_2 injection rate	8.2	kg s^{-1}
Gas production rate	variable	

Table 2. Properties of three-dimensional quarter five-spot domain.

Property	Value	Units
Quarter five spot size	200 x 200 (~10 acres)	m^2
Thickness	50	m
Porosity	0.30	-
Permeability (isotropic)	1.0 x 10^{-12}	m^2
Residual liquid saturation	0.20	
Relative permeability liquid gas	 immobile equal to gas saturation ($k_{rg} = S_g$)	 - -
Molecular diffusivity in gas, liquid	1.0 x 10^{-5}, 1.0 x 10^{-10}	$m^2\ s^{-1}$, $m^2\ s^{-1}$
Temperature	75	˚C
Initial pressure	50	bars
CO_2 injection rate	0.10	kg s^{-1}
Gas production rate	0.009	kg s^{-1}
Final pressure (after 8 years)	67	bars

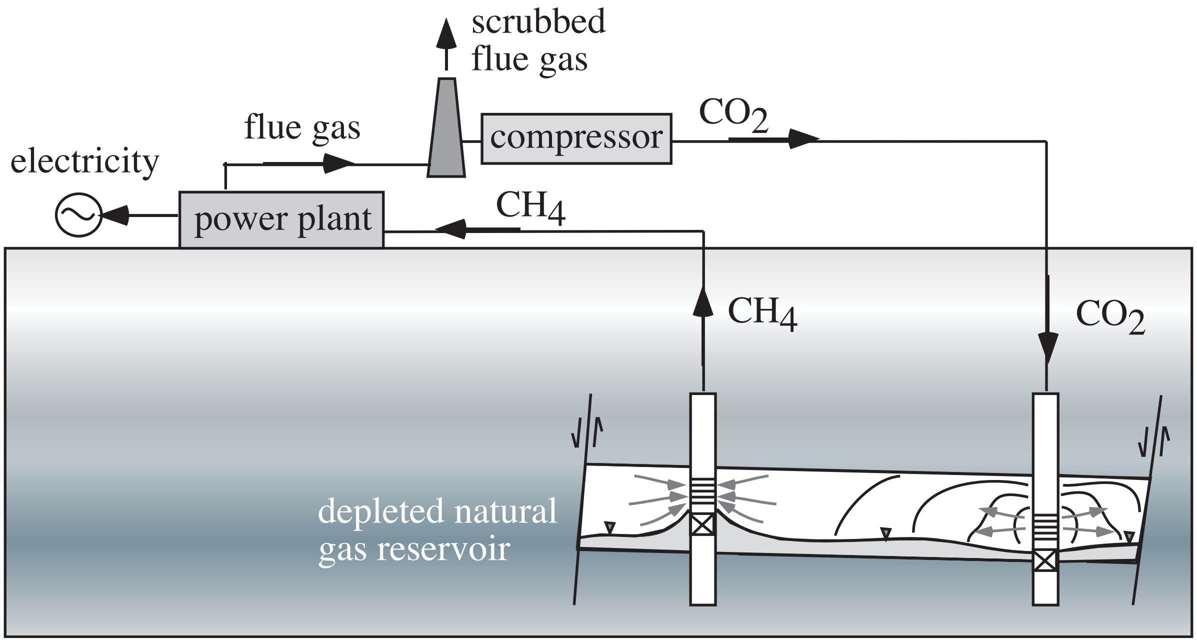

Figure 1. Schematic of a coupled CSEGR system for a gas-fired power plant.

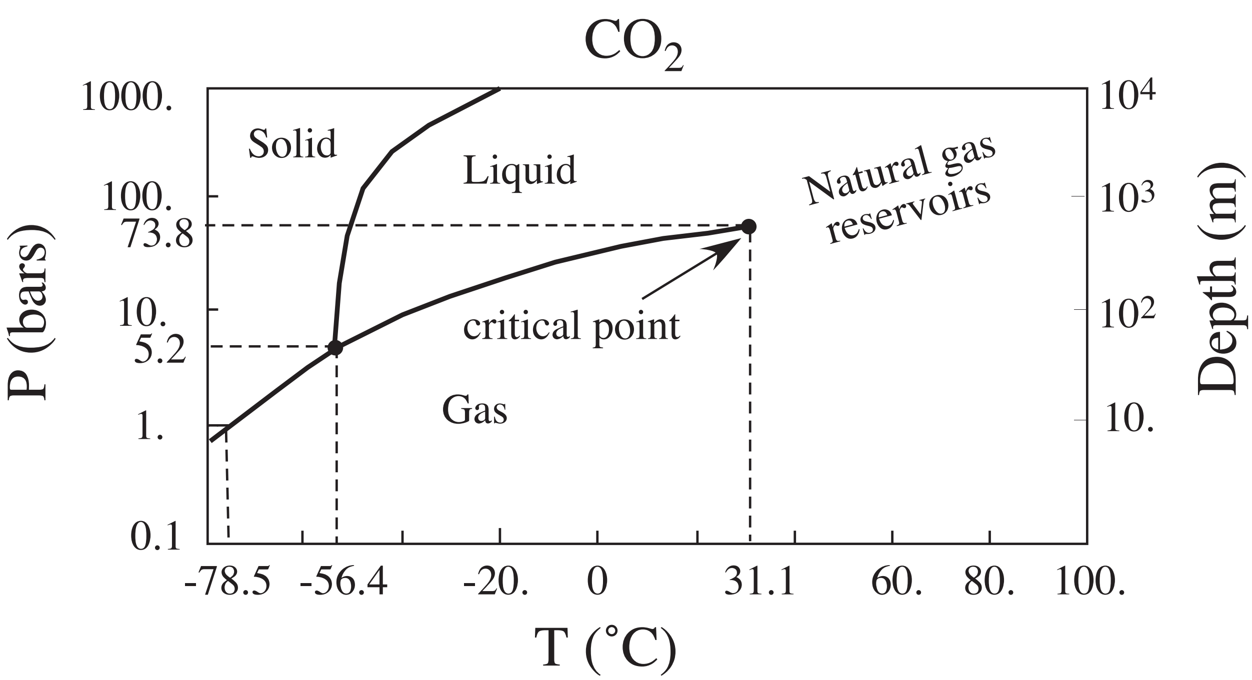

Figure 2. Phase diagram showing CO_2 will normally be supercritical in natural gas reservoirs.

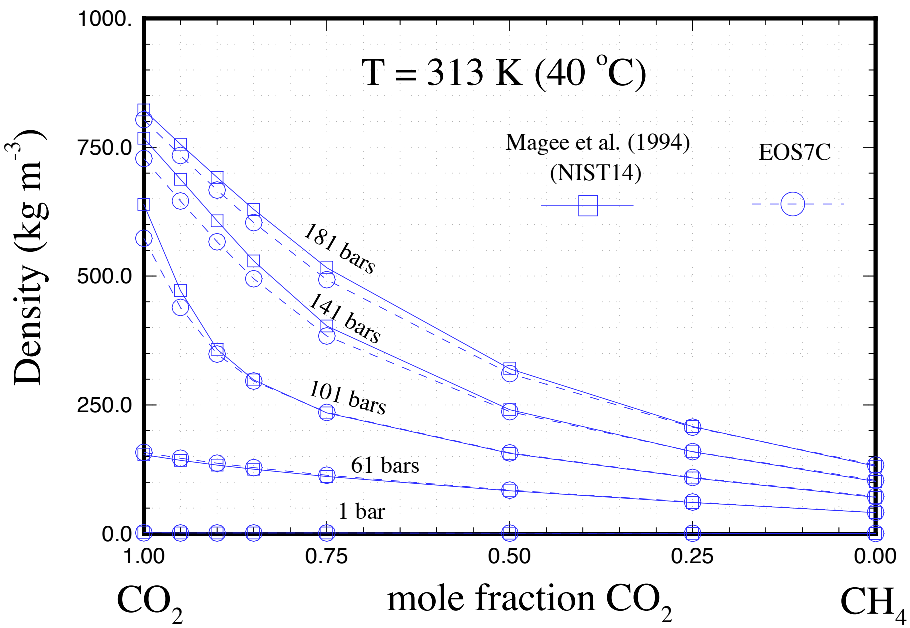

Figure 3. Density at various pressures at 40 ˚C as function of gas composition as calculated from NIST14 and EOS7C.

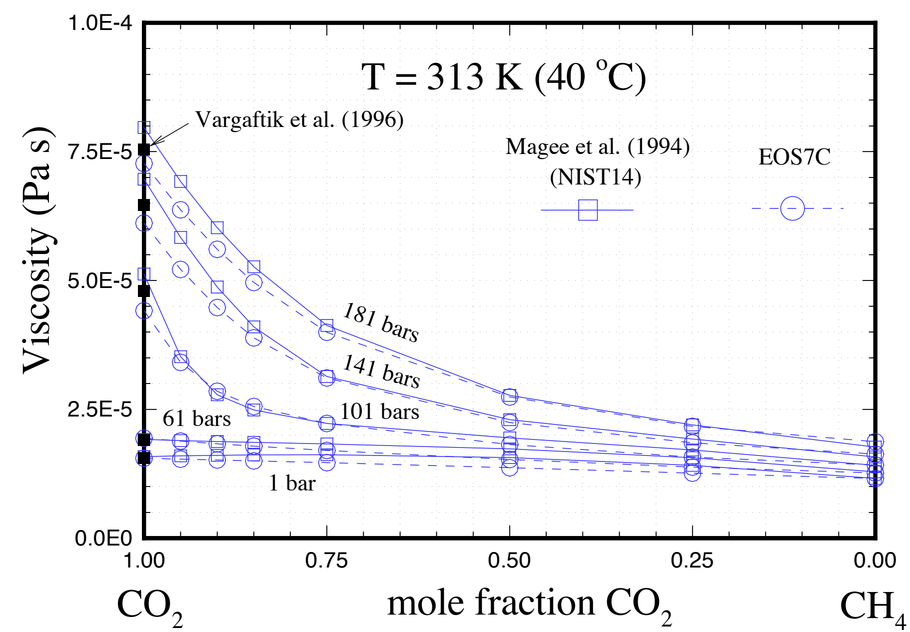

Figure 4. Viscosity at various pressures at 40 ˚C as function of gas composition as calculated from NIST14, EOS7C, and from data for pure CO_2[15].

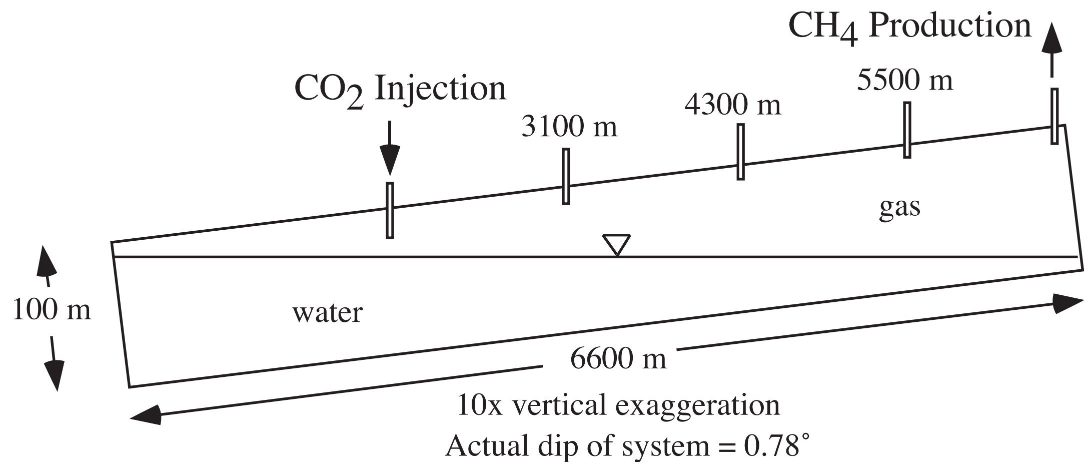

Figure 5. Schematic of two-dimensional Rio Vista simulation domain showing four monitoring locations at Y = 3100 m, 4300 m, 5500 m, and 6500 m.

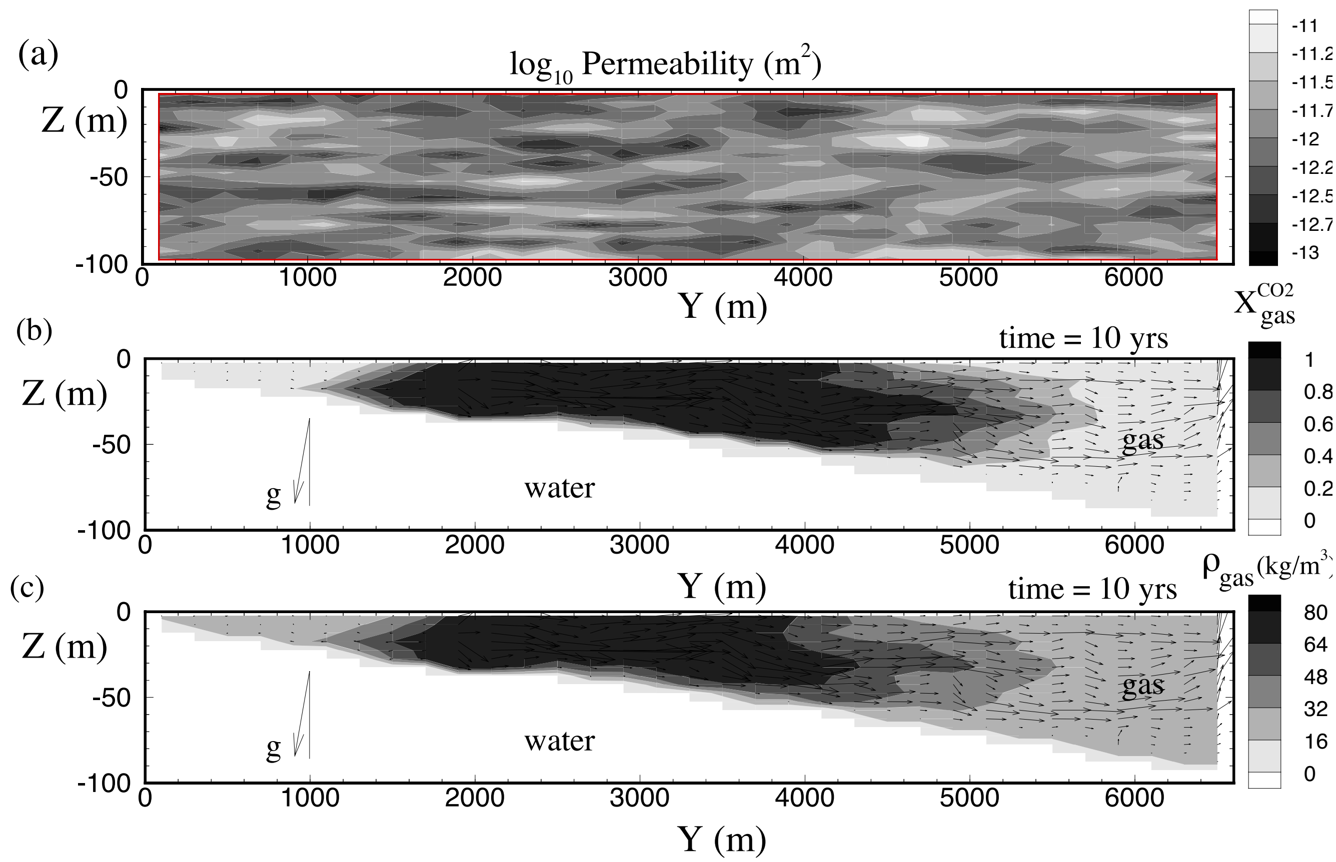

Figure 6. (a) Heterogeneous permeabilty field, (b) mass fraction CO_2, and (c) gas density after 10 years of CO_2 injection at Y = 1900 m with constant pressure at the upper right-hand corner.

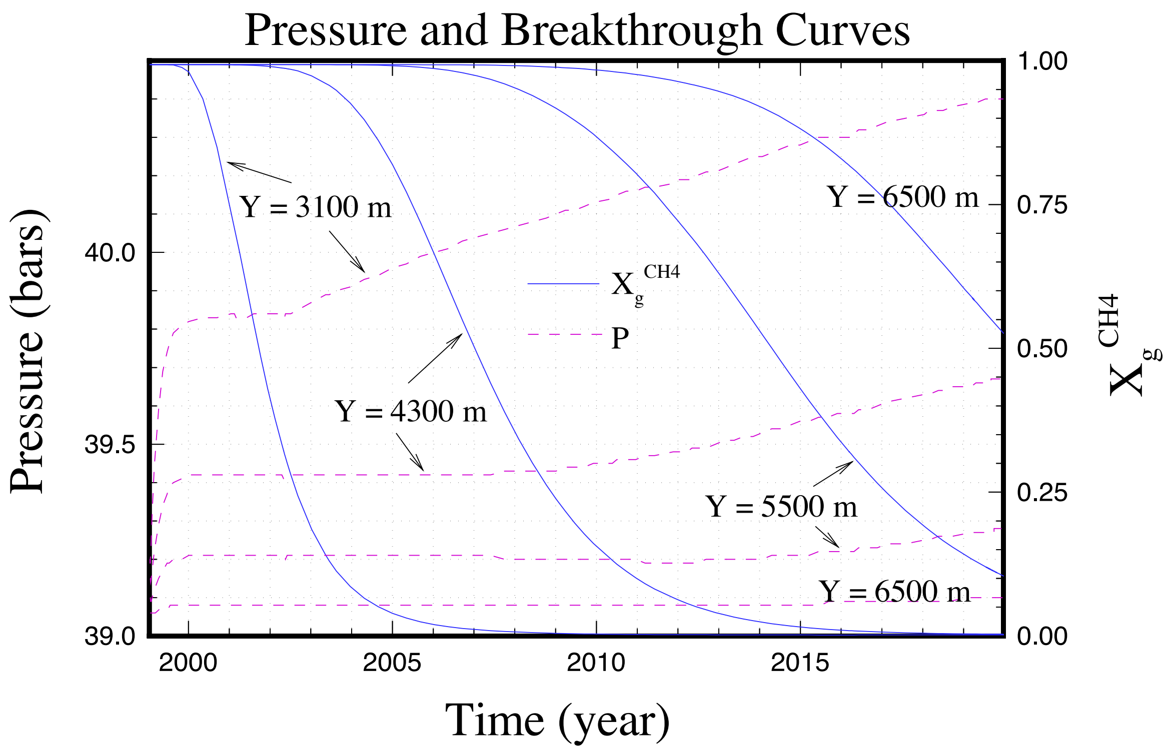

Figure 7. Pressure and breakthrough curves at the four monitoring locations as function of time.

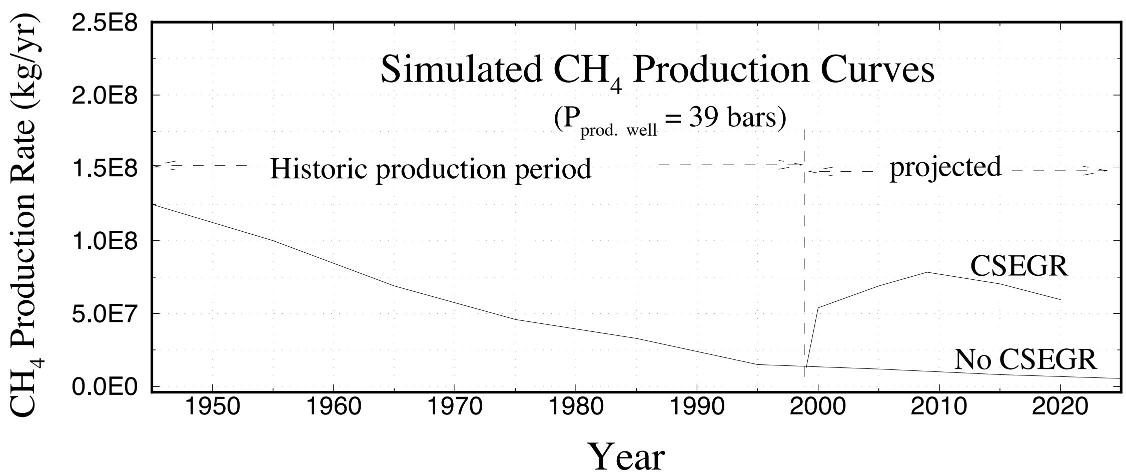

Figure 8. Simulated CH_4 production showing enhancement due to CO_2 injection relative to a projection if no CO_2 injection.

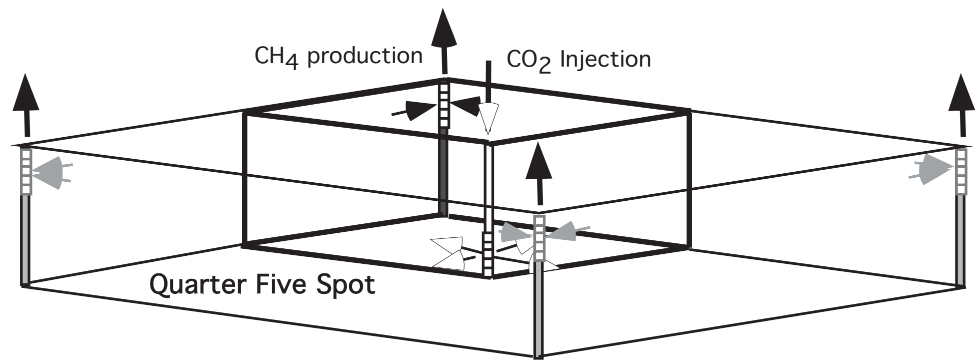

Figure 9. Schematic of the three-dimensional five spot. Heavy lines outline the quarter five spot domain.

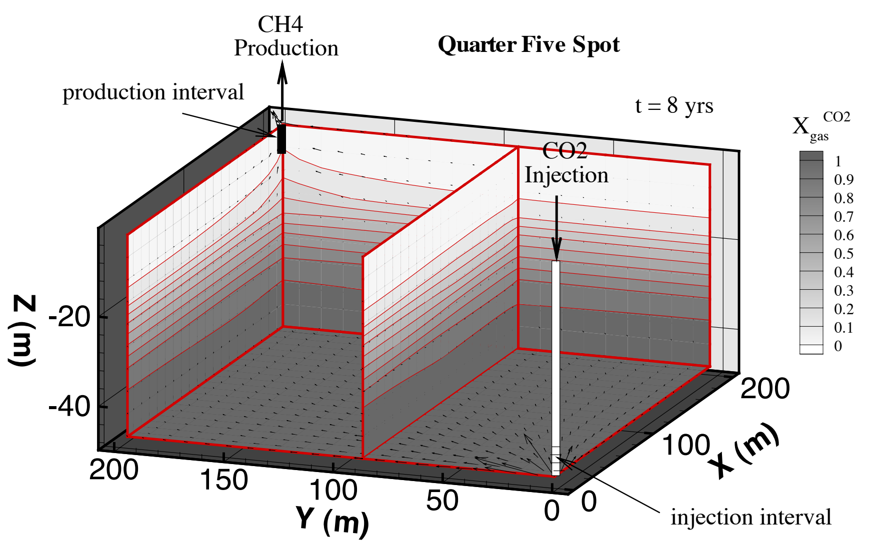

Figure 10. CO_2 mass fraction in the gas after eight years of injection into lower part of reservoir.

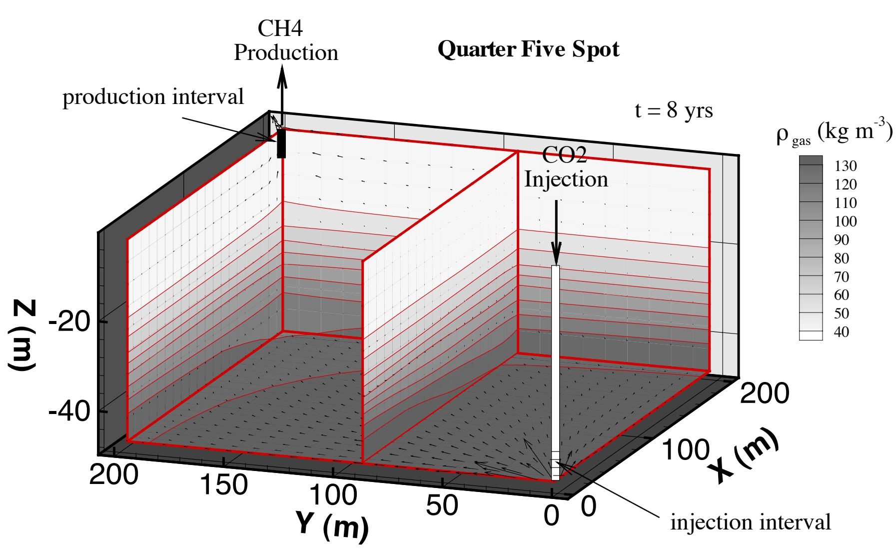

Figure 11. Gas density after eight years of injection into lower part of reservoir.